Radical Pair Kinetics in the Hydrogen Abstraction of Benzophenone Derivatives in Micellar Solutions, Studied by Pulsed Microwave Irradiation

Jonathan R. Woodward[†] and Yoshio Sakaguchi*

RIKEN (The Institute of Physical and Chemical Research), Wako-shi, Saitama, 351-0198, Japan

Received: October 16, 2000; In Final Form: January 19, 2001

The hydrogen abstraction reaction of benzophenones in micellar interiors was studied by the effect of a short, resonant microwave pulse on the recombination kinetics under magnetic fields of approximately 0.3 T. This technique allows all the significant rate constants in the reaction to be determined, in particular the singlet state recombination rate constant, which is very difficult to accurately determine by other techniques. This is determined to be 1.90×10^7 s^{-1} for benzophenone (BP) and 1.83×10^7 s^{-1} for decafluorobenzophenone in sodium dodecyl sulfate (SDS) micelles, indicating that this value is not limited by the rate of spin mixing, and thus that the kinetic approach used is justified. It also indicates that recombination is limited by reencounter frequency and is not dependent upon substitution in the ketyl radical. All kinetic parameters are extracted for each system using a combination of single pulse and pulse shift measurements. Data are also presented for the reactions of BP in SDS solutions of high salt concentration, in polyoxyethylene dodecyl ether (Brij 35), and in hexadecyltrimethylammonium chloride micelles. The rate constants reveal useful information on the effects of the both the micelle interior and the nature of ketyl radical on the recombination kinetics.

Introduction

With the role of free radicals in biological systems becoming increasingly apparent, it remains highly important to have a clear physical picture of the behavior of radicals and, more critically, radical pairs (RPs) in organized systems. As the dynamics of RPs are highly sensitive to the pair's overall spin state, external magnetic fields (both static and oscillatory) are capable of affecting RP behavior. Consequently, the dynamics of RPs have been studied indirectly by the effect of external magnetic fields on the kinetics of radicals (measured using optical techniques),[1] but such optical techniques do not allow discrimination between radicals and RPs. RPs have also been studied by their effect on the polarization of transient electron spin resonance (ESR) spectra.[2] Indeed, in some cases, direct observation of the RP was possible by transient ESR, the RP giving rise to alternating-phase spectra.[3,4] Such techniques yield little kinetic information on the RP due to polarization of the signals. In a previous paper,[5] a new technique, similar to the so-called reaction yield detected magnetic resonance (RYDMR),[6−10] was presented. This technique allows direct observation of RP kinetics, through the application of very short, resonant microwave pulses and detection by transient optical absorption (TROA). Its advantages over pulsed techniques involving microwave detection are 3-fold. First, the use of optical absorption allows measurement of true radical yields unlike ESR techniques, where reaction yields are clouded by the effect of polarization. Second is time resolution. Optical detection means no dead time in the recording of transient signals (which is always present in microwave detection techniques), allowing measurement during the early, critical period of the RP lifetime. Third, measurements can be made in the absence of microwave radiation, allowing data sampling prior to microwave irradiation and allowing the determination of kinetic parameters in a microwave-free environment.

In this paper, we use this new technique to compare the various kinetic parameters in the hydrogen abstraction reaction of benzophenone and its fluorinated derivatives, and the effect of the micellar environment. This technique allows the measurement of the rate of radical recombination, not possible by any other current technique, but also allows other kinetic parameters to be calculated readily and precisely.

Experimental Section

Benzophenone (BP), supplied by Acros, was purified by multiple recrystallizations from a water/ethanol mixture. Sodium dodecyl sulfate (SDS), supplied by Kanto chemicals, was recrystallized from an ethanol/methanol mixture. Polyoxyethylene dodecyl ether (Brij 35) and hexadecyl(cetyl)trimethylammonium chloride (CTAC) were supplied by Kanto chemicals and used as supplied. Decafluorobenzophenone (DFBP) and other benzophenone derivatives were supplied by Aldrich or Acros and used as supplied. Distilled water was purified in an Iwaki UP-100 ultrapure water system by ion exchange and ultrafine filtering and then bubbled with nitrogen for more than 1 h. All samples were prepared by sonication in a nitrogen environment, ensuring that the samples were essentially oxygen free.

SDS was used at a concentration of 80 mM and Brij 35 as a 5% w/w solution, giving a micelle concentration of approximately 1 mM in each case. Benzophenone was used at a concentration of 1 mM to yield, on average, 1 molecule per micelle. DFBP's reduced solubility meant using the highest achievable concentrations, these being 0.2 mM in SDS and 0.13 mM in Brij 35. These concentrations were determined using

* Corresponding Author: Yoshio Sakaguchi. Fax: 81-48-462-4664. E-mail: ysakaguc@postman.riken.go.jp.

[†] Current address: Department of Chemistry, University of Leicester, University Road, Leicester LE1 7RH, England.

10.1021/jp003801x CCC: $20.00
Published on Web 03/29/2001

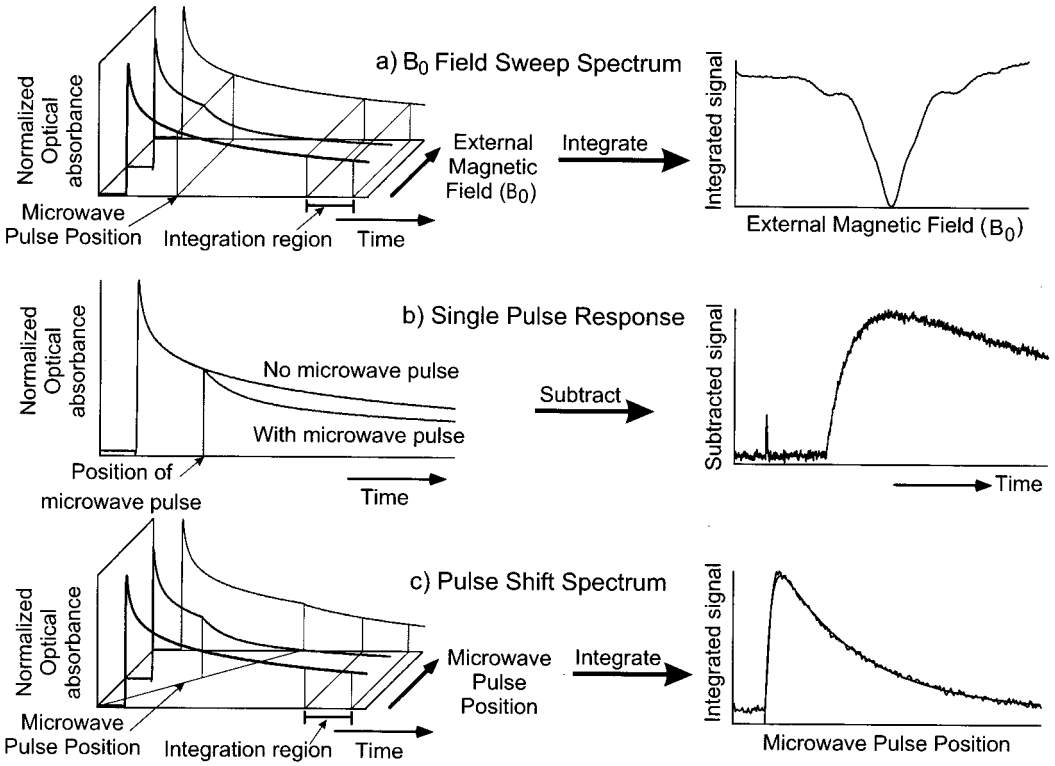

Figure 1. The three modes of spectral acquisition as applied in these experiments. (a) B_0 field sweep spectrum: correlates directly with a transient field sweep time integration EPR experiment. (b) A single pulse spectrum in which TROA curves at high magnetic field are obtained in the presence and absence of resonant microwave pulse and then subtracted. (c) A pulse shift spectrum in which the TROA signal is integrated at times where the signal is due only to escaping radical as the position of the microwave pulse is moved relative to the laser pulse.

UV/vis absorption spectra. Such concentrations were obtained by sonicating DFBP in more concentrated aqueous micellar solutions with subsequent dilution. DFBP is highly insoluble in water, and the chief difficulty in solubilizing it in micelles is kinetic. Thus highly concentrated solutions of micelles are more efficient at allowing DFBP to enter the micelle and are subsequently diluted to give suitable micelle concentrations.

All experiments were performed on flowing samples using the fourth harmonic (266 nm) of a Nd:YAG laser (Spectra-Physics Quanta Ray GCR-3) for excitation. The experimental apparatus has been described previously[5] and was based on a pulsed EPR spectrometer equipped with a 1 kW Litton travelling wave tube amplifier (TWTA) and a rectangular TE102 cavity. Initially, a peristaltic pump was employed for sample flow, although under such conditions oscillations were observed in the TROA signals. Thus all quantitative experiments were performed using gravity or pressure flow techniques. The measurement system[11] consisted of two quartz optical fibers supplying and receiving light along the axis of a quartz cylindrical flow cell along its axis. Light was supplied from a Xenon arc lamp and measured using an ARC SpectraPro 275 monochromator coupled with an HTV R1527 photomultiplier, whose output was digitally recorded on a 500 MHz Tektronix TDS540 oscilloscope. Spectrometer operation and data output were handled by custom written software on a Pentium class microcomputer allowing storage of two-dimensional data for subsequent off-line analysis. The overall time resolution of the measurement system was about 15 ns, the length of the shortest available microwave pulses.

For all experimental systems, three types of experiment were performed: (a) field sweep (B_0) spectra, (b) single microwave pulse transient spectra, and (c) pulse shift spectra. The details of these experiment types are given in Figure 1 and the significance of each is discussed below. For all experiments involving BP, absorption due to the ketyl radical was observed at a detection wavelength of 545 nm (spectra were also recorded at 320 nm to ensure likeness, but were of reduced signal-to-noise ratio). For DFBP experiments, detection took place at 320 nm (here 545 nm spectra were also recorded for comparison and used in the separation of k_{rlx} and k_{esc}; see below). The resonant microwave pulse reduces the absorption in each case, corresponding to a decrease in the concentration of ketyl radicals.

Analysis

Reaction Scheme. Benzophenone and its fluorinated derivatives are excited by UV irradiation and rapidly undergo intersystem crossing (ISC) to yield the triplet state. The triplet state reacts with the micellar environment by hydrogen abstraction to create a triplet radical pair. This process and the subsequent fates of the RP are indicated in the reaction scheme

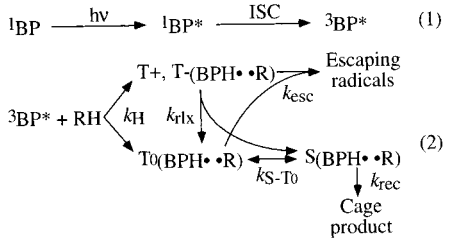

where $h\nu$ corresponds to the laser excitation ($\lambda = 266$ nm); $^3BP^*$ indicates the excited triplet state of BP or a derivative thereof. RH represents a micelle molecule and ^{S,T}(BPH• •R) are the singlet and triplet RPs, the pair members being ketyl and alkyl radicals. The rate constants of hydrogen abstraction (k_H), relaxation between spin states (k_{rlx}), escape of component

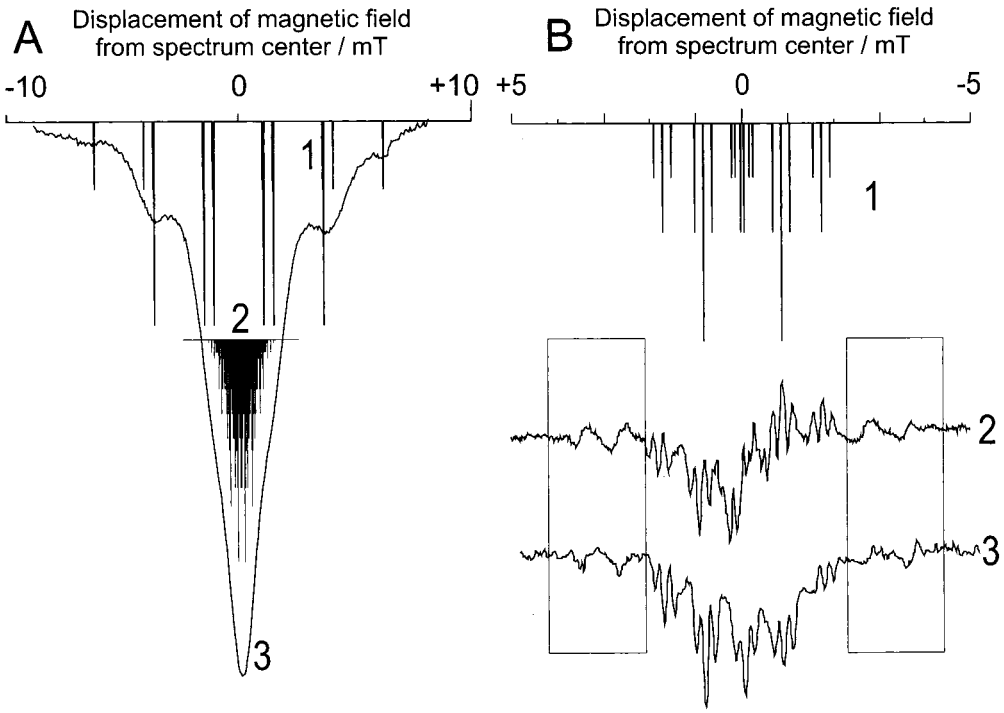

Figure 2. (A) Stick spectrum 1, which represents a simulation of the EPR lines from an SDS micelle derived radical, and stick spectrum 2, one from the benzophenone ketyl radical. Superimposed is a field sweep ODESR spectrum 3 for an optimized 15 ns resonant microwave pulse. All the alkyl lines can be resolved, with those closest to the spectrum appearing as shoulders on the curve. This indicates that a microwave pulse applied at the center of the spectrum is sufficiently narrow to only excite ketyl radicals and not alkyl radicals. The implication is that a 180° pulse is optimum for generating a spin flip in the radical pair. (B) Spectra 2 and 3 illustrate the transient EPR spectra of BP and DFBP in Brij 35, respectively. The stick spectrum 1 is a simulation for the oxyalkyl radical produced from Brij 35, using known hyperfine coupling constants. The additional spectral lines enclosed in boxes cannot arise from the oxyalkyl radical and appear to be due to abstraction from the alkyl region of the micelle.

radicals in a RP (k_{esc}), $S-T_0$ state conversion (k_{S-T_0}), and the recombination rate of singlet RP (k_{rec}) are presented near the corresponding arrows in eq 2. In our systems, we find in all cases that $k_{S-T_0} > k_{rec}$, $k_H > k_{rlx}$, k_{esc}.

The dynamics are governed by the conversion of the RP between singlet and triplet configurations. The external magnetic field (B_0) influences this process, which differs with the specific sublevel of the triplet state (T_+, T_-, and T_0). Under the magnetic field of about 0.3 T of our experiment, $S-T_0$ mixing (k_{S-T_0}) is rapid whereas mixing from T_+ and T_- (k_{rlx}) is impeded by the energy separation of these states due to the Zeeman interaction. The rate constant for $S-T_0$ mixing for BP in SDS calculated using average hyperfine coupling constants is 7.4×10^8 s^{-1} and is dominated by the hyperfine couplings in the alkyl radical (yielding a similar value for DFBP in SDS). This is much faster than any of the other rate processes (in the worst case, it is approximately a factor of 20 faster). Under these conditions, we assume that application of the relaxation mechanism (RM)[12] is justified. It predicts that removal of the RP is controlled by decay from both the rapidly mixed S, T_0 state (hereafter referred to as the mixed state [M]) and the energetically separated T_+ and T_- states ([$T_\pm$]). The rates of these two decay processes can be written as

$$\frac{d[M]}{dt} = k_H[M]_0 e^{-k_H t} - 0.5k_{rec}[M] - k_{rec}([M] - [T_\pm]) \quad (3)$$

$$\frac{d[T_\pm]}{dt} = k_H[T_\pm]_0 e^{-k_H t} - k_{esc}[T_\pm] - k_{rlx}([T_\pm] - [M]) \quad (4)$$

$[M]_0$ and $[T_\pm]_0$ correspond to the $t = 0$ extrapolated values of the [M] and [$T_\pm$] states assuming infinitely fast hydrogen abstraction. Relaxation from the $T_\pm$ states is slower than radical recombination from the singlet state (i.e., $k_{rlx} \ll k_{rec}$), and thus [M] is always smaller than [$T_\pm$] (except under conditions of exceptional polarization: see below). Inversion of the electron spin of either radical pair member will thus lead, on average, to a transfer of population from the $T_\pm$ states to the mixed one. Such a spin flip can be affected by the application of a suitable resonant microwave pulse. As recombination occurs quickly from the mixed state, the effect of such a pulse is to reduce the number of escaping radicals and thus a concomitant reduction in the transient absorbance is observed. Since eqs 3 and 4 are simultaneous differential equations, the solutions are not analytical. Therefore, the detailed analysis of the dynamic behavior of RP requires the comparison between the observation and the numerical solutions. In the present paper and many preceding ones,[13] the coupling between eqs 3 and 4 is neglected because the quasi-stationary value of [M] is nearly zero. With this simplification, the dynamic behavior of [M] and [$T_\pm$] can be described by the combination of exponential functions.

Field Sweep B_0 Spectra and Optimum Pulse Creation. This paper is not concerned with the analysis of field sweep data. References to such work can be found in refs 6−10. It is, however, essential to record accurate B_0 spectra in this system to optimize the measurement conditions.

For each experimental system, B_0 spectra were run to allow selection of resonant microwave pulses. All data contained in this article were obtained using a microwave pulse corresponding to the central resonance in the B_0 spectra, which corresponds to the benzophenone ketyl radical (see Figure 2). In addition, spectra were also recorded for microwave pulses at B_0 values corresponding to the alkyl sidebands in the spectrum. Ensuring that the kinetics of these two processes match guarantees that the radical pair under observation is indeed that consisting of ketyl and micellar alkyl radicals.

TABLE 1: Hyperfine Coupling Constants of Component Radicals

radical	hyperfine coupling constants/mT	ref
BP ketyl in propan-2-ol	4H(o) = 0.323, 4H(m) = 0.123, 2H(p) = 0.364, H(OH) = 0.291	16
DFBP ketyl in propan-2-ol	4F(o) = 0.466, 4F(m) = 0.177, 2F(p) = 0.823, H(OH) = 0.242	17
$C_{11}H_{23}CH{\cdot}OSO_3^-$	H(α) = 1.53, 2H(β) = 2.00	18
$C_{10}H_{21}CH{\cdot}CH_2OSO_3^-$	H(α) = 2.20, 2H(β) = 1.87, 2H(β) = 2.30	19
$C_9H_{19}CH{\cdot}C_2H_4OSO_3^-\cdots C_2H_5CH{\cdot}C_9H_{18}OSO_3^-$	H(α) = 2.14, 4H(β) = 2.55	20
$CH_3CH{\cdot}C_{10}H_{20}OSO_3^-$	H(α) = 2.19, 2H(β) = 2.48, 3H(β) = 2.48	21
$CH_2{\cdot}C_{11}H_{22}OSO_3^-$	2H(α) = 2.20, 2H(β) = 2.76	22
$-OCH{\cdot}CH_2O-$	H(α) = 1.8, 2H(β) = 0.88, 2H($-OCH_2-$) = 0.22	23

After selection of the B_0 value for the microwave pulse, a power (B_1) study is performed by measuring the size of the microwave effect in a single pulse spectrum with increasing microwave field strength. The shortest microwave pulse achievable with the apparatus is 15 ns, and this is thus a fixed parameter in the experiment. Selection of the smallest microwave power that gives rise to the maximum change in escape radical concentration corresponds to a microwave pulse of optimum angle. In most cases the B_1 field strength is considered to be approximately 1 mT, based on the previous experiment.[14] Application of a short, resonant microwave pulse causes an inversion in the spin angular momentum of one of the radical pair members. It is feasible, by choice of field position, to selectively flip either the ketyl or alkyl radical spin. Power broadening and spectral overlap mean, however, that under certain conditions spin inversion is not completely radical selective. For isolated radicals, a 180° pulse gives the maximum conversion between M and $T_\pm$ states. A recent paper by Hore et al.[15] discusses the optimal pulse condition for coupled radicals within a pair and discovers that, for a completely spin-coupled pair, the optimum angle for spin inversion must be 90°. Such a pulse would correspond to excitation across the entire B_0 spectrum. Figure 2A shows the stick spectra for both the benzophenone ketyl radical and SDS alkyl radical. The hyperfine coupling constants of the component radicals are shown in Table 1. These stick spectra are compared with a B_0 spectrum recorded with a typical pulse used for analysis. Hyperfine structure due to the alkyl radical is discernible at all major peak positions, indicating that the actual width of the microwave pulse is sufficiently narrow that if applied at the center of the spectrum, excitation of only the ketyl radical is likely to take place. Thus it would appear that, in this experiment, it is indeed a 180° pulse that is causing maximum conversion between M and $T_\pm$ states, by the flipping of only the ketyl radical spin. Figure 2B, however, illustrates the transient ESR spectra for BP and DFBP in Brij 35. It can be clearly seen that, in the central region, there are spectral lines corresponding to both ketyl and oxyalkyl radicals. As the experiment only requires optimization of conversion of M and $T_\pm$ spin states, the exact pulse angle required is not of concern. This optimization process is performed for each experimental system and whenever physical experimental parameters are altered, ensuring that the microwave pulse is always of the minimum power capable of maximum spin conversion.

Single Microwave Pulse Transient Spectra. Transient absorption signals, $A(t)$'s, in the presence and absence of a resonant microwave pulse were recorded for a series of microwave pulse positions with extensive signal averaging. The reproducibility of the spectra is indicated in the accurate zero subtraction in the premicrowave pulse region. Any signals that gave rise to nonzero subtraction in this region were discarded, such that only reproducible kinetic curves were selected for analysis.

Use of a short microwave pulse, whose action and the system's response to it are temporally well separated, allows simple analysis with direct extraction of the kinetic parameters.

Subtraction of the $A(t)$ curves in the presence and absence of the microwave pulse (as in Figure 1b) gives rise to a curve with a fast exponential rise and a slowly decaying exponential background. These two components correspond to the decay of the enhanced M and reduced $T_\pm$ states, respectively. The fast decay has a rate constant k_{trdec} which, in all cases considered here, is significantly smaller than the rate of $S-T_0$ mixing supporting the single state approximation of $S-T_0$ mixed state. Consequently eqs 3 and 4 hold and the rate constant k_{trdec} can be written in terms of the physically significant rate constants introduced above:

$$k_{\mathrm{trdec}} \approx 0.5k_{\mathrm{rec}} + k_{\mathrm{rlx}} + k_{\mathrm{esc}} \tag{5}$$

$k_{\mathrm{rlx}} + k_{\mathrm{esc}}$ can be calculated from the pulse shift data (see below), and thus the value of the singlet state recombination rate constant k_{rec} is readily obtained from the single pulse spectrum. Experiments were performed at a series of different pulse positions for each system. Although we could derive the information concerning other rate constants from the decaying part, the next measurement is much more suitable for such a purpose.

Pulse Shift Spectra. Pulse shift spectra were obtained as indicated in Figure 1c. For each chemical system, a short time scale and long time scale spectrum was recorded as the pulse shift spectrum consists of a fast rise and a slow decay. The choice of integration region was dependent upon the pulse shift range selected. For long time scale spectra, the experiment becomes technically difficult due to the very small difference between the microwave and nonmicrowave signals at long time. Under such conditions, laser stability and flow rate become critical, as any variation in the signal becomes comparable with or larger than the spectral feature.

Except under the exceptional polarization condition of $[T_\pm](t) - [M](t) = 0$, a population transfer is achieved under application of a microwave pulse at any time after the RP exists. The curve then, corresponds to $[T_\pm](t) - [M](t)$ in the differential eqs 3 and 4, as the population transfer between the $[T_\pm]$ and [M] states is proportional to the population difference between these two states. The initial increase in the spectrum is due to the formation of RPs through the hydrogen abstraction reaction and an increase in the difference in population of the $[T_\pm]$ and [M] states through singlet channel recombination. At later times, the population difference is restored through the relaxation and escape processes. Triexponential fitting of the curve then corresponds to rising rate constants of k_{H} and k_{trdec} and a decay rate constant of ($k_{\mathrm{rlx}} + k_{\mathrm{esc}}$). For this fitting, we already know the value of k_{trdec} from the single pulse study and so the fit need only be performed for two rate constants differing distinctly in magnitude and yielding excellent results. Using this value of ($k_{\mathrm{rlx}} + k_{\mathrm{esc}}$), we can now obtain a value for k_{rec} by subtraction from the single pulse results. Thus the full analysis takes place as follows:

(1) Perform a biexponential fitting to the single pulse subtracted curves. This yields k_{trdec}.

(2) Use this value of k_{trdec} as a fixed parameter in the triexponential fitting to the pulse shift spectrum. This means that the error values quoted for k_H are in addition to those already introduced from k_{trdec}. This also yields ($k_{rlx} + k_{esc}$), which can be used with k_{trdec} to calculate k_{rec}.

(3) Finally, fitting to the original absorbance curves in the absence of microwave pulse is performed using the value of ($k_{rlx} + k_{esc}$) obtained above, where k_{esc} forms the quasi-stationary absorption due to escaping radicals but k_{rlx} does not. With this fitting, individual values of k_{rlx} and k_{esc} can be obtained. The first two fittings define the error in ($k_{rlx} + k_{esc}$), and the final fitting determines the contribution of each. The error value quoted is that for the final fitting process, in which the uncertainty is much larger than any of the previous fittings.

At the shorter wavelength region of the transient absorption of the benzophenone derivatives, there is an additional absorption due to light-absorbing transients (LATs).[24] For the measurements of single pulse response and pulse shift spectra, the difference between the absorbances in the presence and absence of a microwave pulse is calculated. This procedure removes the contribution from any component unaffected by the microwave pulse. Even if the yields of LATs are affected by the microwave field, the kinetics of the pulse shift spectra are unaffected by it, as long as LATs originate from the same RP. This is a practical advantage of our technique. If the yields of LATs are affected by the microwave pulse and their RP dynamics are different from that of the escaping radicals, the shape of single pulse response at the shorter wavelength region is deformed. Since good data for DFBP are obtained from the observation at 320 nm, we require a comparison with the observation at 545 nm. On the other hand, the measurement at 320 nm for BP is auxiliary because the observation at 545 nm does not suffer from a contribution by LATs. For the separation of k_{rlx} and k_{esc}, however, we must use the original absorbance curves. Since the quasi-stationary absorption by LATs disturbs the estimation of k_{esc}, the absorbance at 545 nm is applied even for DFBP.

Results and Discussion

(a) Benzophenone and Decafluorobenzophenone in SDS and Brij 35 Micelles. Figure 3A shows transient optical absorbance curves at 545 nm for BP in SDS in the presence and absence of a 15 ns resonant microwave pulse. Figure 3B shows the subtracted curves along with a biexponential fitting function. Figure 4 shows pulse shift spectra for short and long time scales with triexponential fitting functions, one parameter limited by the results from the single pulse spectra. Similar experiments with suitable time scales were run for all four experimental systems. Using the techniques outlined above, this has allowed complete kinetic analysis in each of these systems. Table 2 gives all the measured parameters for the four systems. The different kinetic parameters determined will be examined individually.

1. Hydrogen Abstraction Rate Constant, k_H. Column 2 of Table 2 gives the hydrogen abstraction rate constants for each chemical system. This is a first-order rate constant for the process indicated in eq 2 and defined in eqs 3 and 4. For both reactants, the hydrogen abstraction rate is greater in Brij 35 micelles than in SDS micelles.

It is important to consider the nature of the micelles before commenting on this value. The structures of the SDS and Brij 35 monomers are indicated below. SDS possesses an anionic

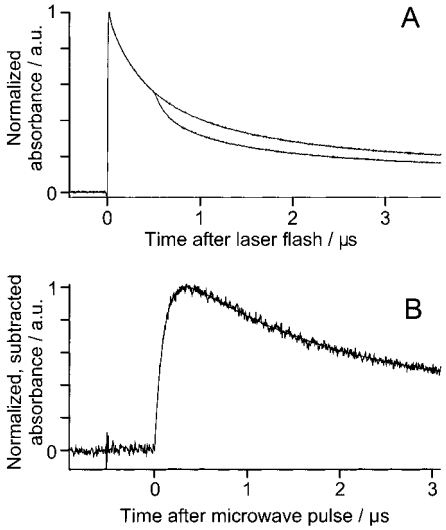

Figure 3. (A) TROA signals for BP in SDS in the presence and absence of a resonant 15 ns microwave pulse applied 500 ns after laser irradiation. (B) The curve obtained by the subtraction of the signals in (A).

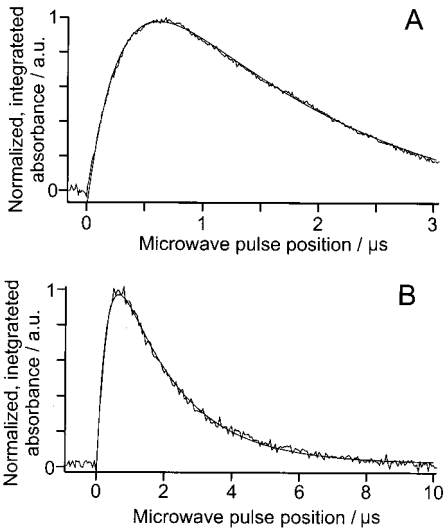

Figure 4. (A) Pulse shift spectrum obtained for a solution of BP in SDS over a 3 μs period. (B) A similar spectrum obtained over a 10 μs period.

headgroup with a 12 carbon atom alkyl chain. Brij 35 possesses an identical alkyl chain, but also has a long polyoxyethylene chain, which forms a neutral hydrophilic headgroup as opposed to the small ionic group in SDS. SDS forms micelles with an aggregation number of about 64 at room temperature,[25] whereas Brij 35 has an aggregation number of about 40 under the same conditions.[26] The rate of hydrogen abstraction ought to be greater from the polyoxyethylene chain than from the alkyl chain, due to the inductive effect of the oxygen atoms. k_H for benzophenone in Brij 35 is much greater than the value in SDS, indicating that significant abstraction is occurring from the polyoxyethylene chain. For DFBP, one might predict a lesser effect due to its much greater hydrophobicity, which might suggest that it resides in the alkyl region and tends to abstract from there. For DFBP, an increase in rate in moving from SDS to Brij 35 is also observed. Although the change is not proportionately as great as for BP, the absolute change in rate constant is greater. Thus the bearing on the extent of abstraction from the polyoxyethylene and alkyl regions is not clear.

Transient EPR spectra were run to determine whether

TABLE 2: Obtained Rate Constants of Benzophenone and Decafluorobenzophenone in Micellar Solutions[a]

chemical system	k_H/s^{-1}	k_{rec}/s^{-1}	k_{rlx}/s-1	k_{esc}/s^{-1}
BP in SDS	$(3.48 \pm 0.06) \times 10^6$	$(1.90 \pm 0.02) \times 10^7$	$(3.3 \pm 0.2) \times 10^5$	$(2.1 \pm 0.2) \times 10^5$
BP in Brij 35	$(8.06 \pm 0.03) \times 10^6$	$(6.01 \pm 0.35) \times 10^6$	$(2.2 \pm 0.2) \times 10^5$	$(1.1 \pm 0.2) \times 10^5$
DFBP in SDS	$(4.33 \pm 0.26) \times 10^7$	$(1.83 \pm 0.01) \times 10^7$	$(8.0 \pm 0.2) \times 10^5$	$(6.2 \pm 0.3) \times 10^4$
DFBP in Brij 35	$(5.16 \pm 0.16) \times 10^7$	$(6.15 \pm 0.02) \times 10^6$	$(3.8 \pm 0.3) \times 10^5$	$(4.9 \pm 0.3) \times 10^4$

[a] k_H, hydrogen abstraction rate constant; k_{rec}, singlet radical pair recombination rate constant; k_{rlx}, longitudinal relaxation rate constant; k_{esc}, escaping rate constant.

TABLE 3: Hydrogen Abstraction Rate Constants of Fluorinated Benzophenones from SDS Micelle

chemical system	k_H/s^{-1}
BP	$(3.48 \pm 0.06) \times 10^6$
3,4-difluoroBP	$(5.70 \pm 0.09) \times 10^6$
2,6-difluoroBP	$(8.30 \pm 0.07) \times 10^6$
2,3,4,5,6-pentafluoroBP	$(1.27 \pm 0.14) \times 10^7$
DFBP	$(4.33 \pm 0.26) \times 10^7$

abstraction takes place from the alkyl region for BP and DFBP in Brij 35. Figure 2B shows the transient EPR spectra of BP and DFBP in Brij 35 along with a stick spectrum for the oxyalkyl radical. It is clear that the oxyalkyl radical is formed in both cases, but there are additional lines (indicated in the boxed regions) that appear to be due to radicals formed by abstraction from the alkyl region. These are present for both BP and DFBP, but the polarized spectra prevent any direct comparison of the proportion of alkyl/polyoxyethylene abstraction for the two reactant molecules. Thus the position of the DFBP molecule cannot be readily concluded from these data, although the experiments reveal, significantly, that both BP and DFBP extract from both regions of the Brij 35 micelle. This seems to indicate that BP and DFBP triplets and ketyl radicals experience similar local environments on creation and removal. This is in good agreement with the variation in k_{rec} (see next section).

Comparison of reactants reveals the much greater reactivity of DFBP toward hydrogen abstraction relative to BP. BP and DFBP have the same triplet energy, and both triplets have an $n\pi^*$ configuration. The difference in reactivity has been attributed to (i) the electron affinity of the fluorine atoms making the carbonyl oxygen more electrophilic by delocalization of the electron cloud into the phenyl ring[27] and (ii) the perfluoro effect which stabilizes the σ bond and increases the strength of the O−H bond being formed.[28−30] In fact, a series of fluorinated benzophenones were examined in SDS solution and, as indicated in Table 3, the hydrogen abstraction rate constant increased with increasing degree of fluorination.

It can be seen that, for the two disubstituted benzophenones, hydrogen abstraction is more rapid in the 2,6-isomer. Again, this is due to the increased polarity in the $n\pi^*$ triplet state.

2. Singlet-State Recombination Rate Constant, k_{rec}. The measurement of this parameter was the driving force behind this study, as this value cannot currently be obtained by any other experimental means. Usually the estimation of this value is done by analyzing transient absorption curves without microwave pulses. The high yield of escaping radical or the overlap of the T−T absorption signal makes such an estimation very difficult. The sense of this rate constant is quite clear in that we are quoting the rate at which singlet radical pairs recombine within the micelle and thus the rate constant is first order. Column 3 of Table 2 gives the values obtained for the systems studied.

Experimental parameters must be thoroughly investigated and fitting functions carefully considered to extract the correct values from these systems. Particularly in the DFBP systems, where secondary reaction with light-absorbing transients (LATs)[24] can lead to erroneous values, great attention must be paid to flow rate and laser repetition rate. Early (unpublished) experiments indicated differences between BP and DFBP values in like micelles, although it is clear from the above table that this is not the case.

The fact that there is no difference in singlet recombination rate for BP and DFBP is a significant one (k_{rec} was found to be constant for all of the fluorinated benzophenones listed in Table 3). The recombination rate is subject to three factors: the rate of $S-T_0$ mixing, the re-encounter frequency, and the probability of reaction during a radical pair encounter in the singlet state, effectively a steric parameter. One would expect the final parameter to be equal, or very similar, for BP and DFBP as they are sterically similar species. For a given micelle, the re-encounter frequency should be the same, and thus the only difference we might expect between BP and DFBP would come from a difference in $S-T_0$ mixing frequency. The fact that we observe no difference, within experimental error, is important in that it implies that $S-T_0$ mixing is very rapid relative to re-encounter frequency—something we assumed when applying this kinetic model. The hyperfine coupling constants for the BP and DFBP ketyl radicals are given in Table 1. Although one would expect a greater rate of spin mixing for DFBP than for BP, due to the greater hyperfine coupling constants, no effect on k_{rec} is observed, implying that the kinetic approach used is justified and that $S-T_0$ mixing is much more rapid than the kinetic processes in these systems.

The fact that k_{rec} is unchanged for BP and DFBP has two implications. The first is that the exponential model is a reasonable one for this analysis in that, although the interface to the bulk water affects the diffusion of the BP and DFBP ketyl radicals differently, due to their differing hydophobicity, there is no effect observed on the recombination. This agrees with the effect of micelle on k_{rec} (discussed below). The second is that the local environment for recombination is very similar for both ketyl radicals, which is particularly important in the case of Brij 35. This agrees with the comments on hydrogen abstraction (see above).

Our technique also allows the calculation of k_{rec} at varying time points after radical creation. The above values were calculated as an average of the values sampled at 100, 250, 500, 750, and 1000 ns after laser excitation. There is some evidence for variation in the value of k_{rec} with time. This is currently under further investigation, and if it provides fruitful information, it will be discussed in a future publication.

The value of k_{rec} is clearly affected by the micellar environment. Recombination occurs much more quickly in SDS than in Brij 35. If the re-encounter were simply diffusion controlled, one would expect the re-encounter rate constants to scale inversely with the microviscosity of the micelle. If, however, singlet recombination is highly inefficient, recombination will take place over a longer time scale, which is also affected by the microreactor volume and the recombination efficiency. Many studies have attempted to estimate the internal microviscosity

of SDS,[31,32] and a value of 8−12 cP is commonly used at room temperature. For Brij 35, there is much less data, although a recent paper by Zana[33] using the fluorescence emission of 1,3-dipyrenylpropane gives a microviscosity ratio for SDS:Brij 35 of 1:3.3 at 25 °C. The observed ratio of the rate constants is 3.2:1, in excellent agreement. If the recombination were dependent also on the microreactor volume, a larger discrepancy between the SDS and Brij 35 values would be expected, due to the much greater size of the Brij 35 micelles. It would appear then that recombination is diffusion controlled and determined primarily by the internal viscosity of the micelle, although it is important to remember that the microviscosity data in the literature is probe specific and the exact nature of the micelle interior is not clear. It appears that the micellar barrier does not influence the recombination process, although one might have suspected otherwise.

In an attempt to learn a little more about the effects of the micelle environment on k_{rec}, experiments were performed in CTAC, a cationic micelle, and also in salted SDS solutions where the micelle shape and size are significantly altered. These results are discussed in section b below.

It is also interesting to note that for all the systems considered, BP in SDS is the only one in which the singlet state recombination rate constant is greater than the hydrogen abstraction rate constant. This is manifest in the pulse position curve, which shows virtually no dependence on the value of k_{rec}. This is because the curve effectively becomes limited by the rate of hydrogen abstraction. This would bear significantly on attempts to measure the hydrogen abstraction and recombination rates using only optical absorption techniques, leading to large errors in the values. For large abstraction rate constants, the fitting to optical absorption curves should yield more accurate estimates of the recombination rate, but clearly large errors are likely to be observed for BP in SDS. Therefore, the use of short microwave pulses is invaluable in making the comparisons described above.

3. Longitudinal Relaxation Rate Constant, k_{rlx}. The value of k_{rlx} can be expressed in terms of intermolecular (k_{ab}) and intramolecular relaxation terms (k_r, r = a, b) for radical pair members a and b.

$$k_{rlx} = k_{ab} + k_a + k_b \tag{6}$$

where

$$k_{ab} = \left|\frac{V_{ab}}{\hbar}\right|^2 \frac{2\tau_{ab}}{1 + \omega^2 {\tau_{ab}}^2} \tag{7}$$

$$k_r = \left|\frac{V_r}{\hbar}\right|^2 \frac{2\tau_r}{1 + \omega^2 {\tau_r}^2} \tag{8}$$

Here, V_{ab} is the spin−spin dipole interaction between the radical pair members and V_r is derived from the anisotropic Zeeman and hyperfine coupling terms within radical r. τ_{ab} and τ_r are the rotational correlation times. This means that we expect to observe both solvent and fluorination effects on the relaxation rate. Once again we quote a first-order rate constant as we are concerned with the rate at which radical pairs (as a whole) relax. Column 4 of Table 2 gives the values obtained experimentally.

As expected, the relaxation rate is faster for DFBP than for BP (in both micelles). There are no literature data on the values of the anisotropic hyperfine coupling constants for aromatic hydrogen and fluorine atoms. The best comparison available is between perfluoro-1,3-butadiene and 1,3-butadiene as an example of fluorine and hydrogen atoms attached to conjugated systems. For perfluoro-1,3-butadiene cation radical in $CClF_2$-$CClF_2$ at 77 K,[34] the anisotropy of F is very large. The anisotropic hyperfine coupling constants of the four F atoms attached to C1 and C4 are 10.64 mT, approximately 0 mT, and approximately 0 mT. The anisotropic *g* values are reported as 2.0026, 2.0056, and 2.0056. For the 1,3-butadiene cation in CCl_3F at 77 K,[35] the ESR spectrum is broadened by the anisotropic contribution, but the smaller (0.02 mT) splitting by the H atoms attached to C2 and C3 is still observable. No anisotropy in the *g* values is observed. It is reasonable to suggest that the anisotropic hyperfine contribution from DFBP should be greater than that of BP, in agreement with the experimental data.

In changing from SDS to Brij 35, we see a decrease in k_{rlx} for both BP and DFBP. There are three factors that are likely to affect the rate of relaxation: any change in the anisotropic hyperfine couplings in the counter radical, the change in the internal viscosity, and the distance between the component radicals of a pair. The microviscosity of the Brij 35 micelle is much greater than that of SDS (see above), and this should cause a decrease in the relaxation rate through the rotational correlation time. Similarly, the larger size of Brij 35 micelle seems to increase the interradical distance, which also causes a decrease in the relaxation rate through the dipole−dipole interaction. These expectations agree with the experimental data. Since the ketyl radicals from BP and DFBP move similarly in each micelle as described in the previous section, these two factors are not the origins of the difference between BP and DFBP. The change in the anisotropic *g* values and hyperfine coupling constants of the micelle derived radical is expected to be smaller than for the replacement of H with F in the ketyl radical. It is significant to note that the change in moving from SDS to Brij 35 is increased for DFBP over BP. Again it is difficult to comment on this based on the lack of information on the viscosity variation within the micelle, the extent of abstraction from alkyl and oxyalkyl parts, and the difference in anisotropic *g* values and hyperfine coupling constants and *g* values of the alkyl and oxyalkyl radicals.

4. The Radical Escape Rate Constant, k_{esc}. The value of k_{esc} represents the absolute escape rate of radicals from the micellar cage. This value is likely dominated by the escape of ketyl radicals through the interface of the micelle (i.e., the Stern layer for ionic micelles) and into bulk solution, although it is possible that there is contribution from the loss of the micelle derived radical. The values obtained for the systems studied are indicated in column 5 of Table 2.

There is a very significant reduction in the escaping rate in moving from BP to DFBP. This has been commented on previously[13] and has been attributed to the much greater hydrophobicity of DFBP relative to BP. Assuming unit permeability of the Stern layer, the rate of ketyl radical escape from the micelle can be estimated at 4.0×10^7 s^{-1} for BP in SDS micelles (using micellar dimension data from ref 36, the microviscosity described previously, and a BP radius of 0.5 nm), although this is rather approximate. This gives a reduction factor of 190 for BP and 363 for DFBP. For SDS, the rate at which monomers exit the micelle is 1.0×10^7 s^{-1},[25] which, along with the aggregation number for SDS, means that the rate of loss of micelle derived radicals ought to be about 1.6×10^5 s^{-1}. This figure seems a little larger than the expected. As described at the beginning of this section, the main part of k_{esc} is attributable to the escape of BP ketyl radical for the cases of BP. On the other hand, we may assume that the main part of k_{esc} is

dominated by the escape of the micelle derived radical for the cases of DFBP. Therefore, the above value is 3 times larger than our observation, which may not be serious considering the much lower time resolution (>1 μs) of the above measurement. Substituting the above value for k_{esc} has only a small effect on k_{rlx} and does not affect the discussion in the previous section.

Using this approach, we can also estimate the escaping rates of BP ketyl radical in SDS and Brij 35 to be 1.5×10^5 and 0.6×10^5 s^{-1}, respectively. The ratio is 2.5, which is similar to the ratio (~3) of k_{rec} in SDS and Brij 35. If the potential at the interface to the bulk water is similar in SDS and Brij 35 micelles, it is safe to assume that the escape process of the BP ketyl radical is controlled by the total mobility (size and viscosity), as for k_{rec}. In this case, the resemblance of the ratios is reasonable. In comparison, using micelle dimension data from ref 37, using Zana's microviscosity data above, and again assuming unit permeability, the rate of BP ketyl radical escape from Brij 35 can be estimated at 2.3×10^6 s^{-1}. This is more than an order of magnitude lower than for SDS micelles. There is, again, qualitative agreement in the micelle effect on escape rate, although this value would imply that both the micellar dimensions and internal viscosity, along with the permeability of the interface to the bulk water, affect the escaping rate. For DFBP, with its high hydrophobicity, we would expect a smaller difference between SDS and Brij 35 than for BP, as the internal properties of the micelle are less important relative to the interface permeability. Also, the low solubility of the DFBP ketyl radical in the water layer means that the escaping rate will more likely reflect the escape of the micelle derived radical, leading qualitatively to the same effect. This is reflected in the experimental data. It should also be noted that values for k_{rlx} and k_{esc} are separated by fitting to the optical absorption curves, and are thus more susceptible to error than the other rate constants, particularly for large differences in the relaxation and escape rates (i.e., for the DFBP systems).

(b) Benzophenone in Other Micelles. (*1*) *Benzophenone in CTAC Micelles.* Although the rate constants discussed above suggest that the ionic or nonionic nature of the micelle surface does not significantly affect the kinetics of the contained radicals, it is prudent to examine a cationic micelle to ensure that no unusual effects are observed. Hexadecyltrimethylammoium chloride has the advantage of possessing an alkyl chain similar to that of SDS, which aids comparison. For CTAC, the headgroup is a cationic ammonium moiety and the chain length is longer than SDS, consisting of 16 carbon atoms. Also, the aggregation number of CTAC at the concentration and temperature used is approximately 105.[38] This serves to make CTAC micelles larger than SDS ones with a greater internal viscosity. Based on the literature aggregation number, a CTAC concentration of 105 mM was used to create micelles at a concentration of 1 mM, for direct comparison with the SDS and Brij 35 systems. Thus, in comparing CTAC with SDS, we might expect a slower recombination rate, due to the greater viscosity, and a very similar rate of hydrogen abstraction due to the very similar alkyl chain. The experimentally determined values are $k_{rec} = (1.02 \pm 0.02) \times 10^7$ s^{-1} and $k_H = (3.22 \pm 0.06) \times 10^6$ s^{-1}.

Indeed, the rate constants change in roughly the way we expect based on the comparison between SDS and Brij 35. The microviscosity of CTAC has been measured to be approximately twice that of SDS,[31] and thus the measured recombination rate scales excellently with the expected effect of viscosity on diffusion controlled recombination. Hydrogen abstraction rate agrees excellently with that in SDS, given the very similar alkyl chain.

(2) BP in Salted SDS Micelles. SDS micelles change their properties considerably in solutions of high ionic strength. When the counterion concentration is increased beyond some critical value, the aggregation number increases very strongly and values from 250 to 1000 (depending on the measurement technique) are claimed for solution with a salt concentration of 0.8 M.[39−42] The increase in aggregation number at high concentrations is known as the sphere-to-rod transition and results in a change in the shape of the micelle to a rodlike form. The desire to determine k_{rec} in this system is based on the fact that the counter radical should be identical to nonsalted solutions, but the properties of the micelle are changed. Only microreactor volume and internal viscosity are likely to change from the salt-free solution.

Experiments were performed using the same concentration conditions as for the nonsalted BP/SDS solutions, with the addition of 1 M NaCl. Clearly this is not ideal, as the occupancy of BP in the micelles must necessarily increase in the micelles. Regardless, experiments were performed under these conditions. A value of k_{rec} was determined under these conditions to be $(8.51 \pm 0.02) \times 10^6$ s^{-1}, which is considerably lower than the value in salt-free SDS. The microviscosity of SDS has been shown to increase considerably on undergoing the sphere to rod transition,[43] which agrees with the observed value of k_{rec} and the earlier discussion. The rate of hydrogen abstraction was unchanged from regular SDS solutions at $(3.01 \pm 0.11) \times 10^6$ s^{-1} as expected.

Conclusions

The technique of pulsed resonant microwave irradiation proved highly successful in elucidating the recombination kinetics of BP derivatives in micellar solution. Experimental reproducibility was very high, giving nearly identical rate constants for the BP/SDS system for a series of repeat experiments.

For the systems studied, the singlet state recombination rate constant was found to be largely affected by the dimensions and nature of the micellar interior, with no influence observable due to substitution in the phenyl groups. Other rate constants in the system were found to vary as expected with ketyl and micelle parameters and in general were indicative of the power of the technique in providing a clear kinetic analysis.

One of the strong advantages of the technique is the use of the pulse shift experiment. These experiments have revealed that this measurement is an effective one, as long as there is a reasonable degree of radical escape from the micelle. In systems that show large magnetic field effects on the recombination process, but small effects on the escaping radical yield, pulse shift measurements would be difficult to perform due to the small change in signal at long times, even when the effect of the microwave pulse is maximum. To some extent, the micellar environment is an ideal one, in that it constrains the radical pair sufficiently to extend its lifetime to observable time scales, but it allows sufficient separation of the pair to allow the observation of spin effects in the escaping radicals and products.

Acknowledgment. J.R.W. is grateful to RIKEN for awarding him a collaborative scientist position in the Molecular Photochemistry Laboratory.

References and Notes

(1) Nagakura, S.; Hayashi, H.; Azumi, T. *Dynamic Spin Chemistry* Kodansha/Wiley: Tpkyo and New York, 1998.

(2) McLauchlan, K. A.; Yeung, M. T. *Spec. Period. Rep. Chem. Soc.* **1994**, *14*, 32.

(3) Sakaguchi, Y.; Hayashi, H.; Murai, H.; I'Haya, Y. J. *Chem. Phys. Lett*. **1977**, *47*, 304.
(4) Closs, G. L.; Forbes, M. D. E.; Norris, J. R. *J. Phys. Chem.* **1987**, *91*, 3592.
(5) Sakaguchi, Y.; Astashkin, A. V.; Tadjikov, B. M. *Chem. Phys. Lett*. **1997**, *280*, 481.
(6) Frankevich, E. L.; Prisyupa, A. I.; Leshin, V. I. *Chem. Phys. Lett*. **1977**, *47*, 304.
(7) Anisimov, O. A.; Grigoryants, V. M.; Molchanov, V. K.; Molin, Yu. N. *Chem. Phys. Lett*. **1979**, *66*, 265.
(8) Norris, J. R.; Bowman, M. K.; Budil, D. E.; Tang, J.; Wraight, C. A.; Closs, G. L. *Proc. Natl. Acad. Sci. U.S.A.* **1982**, *79*, 5532.
(9) Okazaki, M.; Shiga, T. *Nature* **1986**, *323*, 230.
(10) Grant, A. I.; McLauchlan, K. A.; Nattrass, S. R. *Mol. Phys*. **1985**, *55*, 557.
(11) Astashkin, A. V.; Sakaguchi, Y. *J. Phys. Chem*. **1997**, *106*, 9190.
(12) Hayashi, H.; Nagakura, S. *Bull. Chem. Soc. Jpn*. **1984**, *57*, 322.
(13) Igarashi, M.; Meng, Q.-X.; Sakaguchi, Y.; Hayashi, H. *Mol. Phys*. **1995**, *84*, 943.
(14) Tadjikov, B. M.; Astashkin, A. V.; Sakaguchi, Y. *Chem. Phys. Lett.* **1998**, *283*, 179.
(15) Timmel, C. R.; Fursman, C. E.; Hoff, A. J.; Hore, P. J. *Chem. Phys*. **1998**, *226*, 271.
(16) Wilson, R. *J. Chem. Soc. B* **1968**, 84.
(17) Sargeant, F. P.; Bailey, M. G. *Can. J. Chem.* **1973**, *51*, 3211.
(18) Zeldes, H.; Livingston, R. *J. Chem. Phys*. **1966**, *44*, 1245.
(19) Norman, R. O. C.; Storey, P. M.; West, P. R. *J. Chem. Soc. B* **1970**, 1087.
(20) Paul, H.; Fischer, H. *Helv. Chim. Acta* **1973**, *56*, 1575.
(21) Krusic, P. J.; Kochi, J. K. *J. Am. Chem. Soc*. **1968**, *90*, 7155.
(22) Fischer, H. *J. Phys. Chem*. **1969**, *73*, 3834.
(23) Sakaguchi, Y.; Hayashi, H.; *Symposium on Molecular Science*; Kyoto, Sept 14, 1992; Abstract No. 3bp29.
(24) Scaiano, J. C.; Abuin, E. B.; Stewart, L. C. *J. Am. Chem. Soc*. **1982**, *104*, 5673.
(25) Aniansson, E. A. G.; Wall, S. N.; Almgren, M.; Hoffman, H.; Kielmann, I.; Ulbricht, W.; Zana, R.; Lang, J.; Tondre, C. *J. Phys. Chem*. **1976**, *80*, 905.
(26) Becker, P. *J. Colloid Interface. Sci*. **1962**, *17*, 325.
(27) Kebarle, P.; Chowdhury, S.*Chem. Rev*. **1987**, *87*, 513.
(28) Brundle, C. R.; Robin, M. B.; Kuebler, N. A.; Basch, H. *J. Am. Chem. Soc*. **1972**, *94*, 1451.
(29) Yim, M. B.; Wood, D. E. *J. Am. Chem. Soc*. **1976**, *98*, 2053.
(30) Kobayashi, Y.; Kumadaki, I. *Acc. Chem. Res*. **1981**, *14*, 76.
(31) Emert, J.; Behrens, C.; Goldenberry, H. *J. Am. Chem. Soc.* **1979,** *101*, 771 and references therein.
(32) Turro, N. J.; Aikawa, N.; Yekta, A. *J. Am. Chem. Soc*. **1979**, *101*, 772 and references therein.
(33) Zana, R. *J. Phys. Chem. B* **1999**, *103*, 9117.
(34) Shiotani, M.; Kawazoe, H.; Sohma, J. *Chem. Phys. Lett*. **1984**, *115*, 254.
(35) Shida, T.; Egawa, Y.; Kubodera, H. *J. Phys. Chem*. **1980**, *73*, 5973.
(36) Tanford, C. *J. Phys. Chem*. **1972**, *76*, 3020.
(37) Tanford, C.; Nozaki, Y.; Rhode, M. F. *J. Phys. Chem*. **1977**, *81*, 1555.
(38) Kalyanasundaram, K. *Photochemistry in Microheterogeneous Systems*; Academic Press: Orlando, 1987.
(39) Chen, J. M.; Su, T. M.; Mou, C. Y. *J. Phys. Chem*. **1986**, *90*, 2418.
(40) Nguyen, D.; Bertrand, G. L. *J. Phys. Chem*. **1992**, *96*, 1994.
(41) Stephany, S. M.; Kole, T. M.; Fisch, M. R. *J. Phys. Chem*. **1994**, *98*, 11126.
(42) Rawat, S.; Chattopadhyay, A. *J. Flouresc*. **1999**, *9*, 233.
(43) Miyagashi, S.; Asakawa, T.; Nishida, M. *J. Colloid Interface. Sci*. **1987**, *115*, 199.